Article

Cell Reports

Vitamin D3 Induces Tolerance in Human Dendritic Cells by Activation of Intracellular Metabolic Pathways

Graphical Abstract

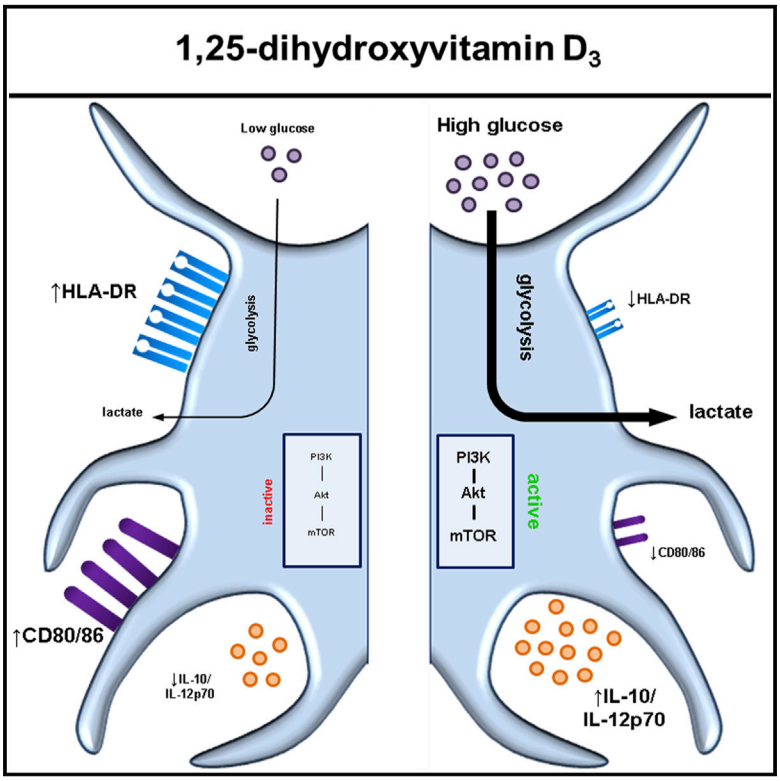

Authors

Gabriela Bomfim Ferreira, An-Sofie Vanherwegen, ..., Lut Overbergh, Chantal Mathieu

Correspondence

lut.overbergh@med.kuleuven.be

In Brief

Ferreira et al. show that the active form of vitamin D, 1,25-dihydroxyvitamin D_3, promotes tolerogenic human monocyte-derived dendritic cells via the activation of glucose metabolism in these cells. Specifically, glucose availability and glycolysis, controlled by the PI3K/Akt/mTOR pathway, dictate the induction and maintenance of the tolerogenic DC phenotype and function.

Highlights

- 1,25(OH)2D3 triggers transcriptionally mediated metabolic reprogramming in human DCs
- 1,25(OH)2D3 induces oxidative and glycolytic metabolic pathways in human DCs
- Glucose, glycolysis, and PI3K/Akt/mTOR are essential for the 1,25D3-DC function
- Other tolerance-inducing agents are not dependent on PI3K/Akt/mTOR signaling

Accession Numbers

GSE56490

Ferreira et al., 2015, Cell Reports *10*, 711–725
February 10, 2015
http://dx.doi.org/10.1016/j.celrep.2015.01.013

Cell Reports
Article

Vitamin D3 Induces Tolerance in Human Dendritic Cells by Activation of Intracellular Metabolic Pathways

Gabriela Bomfim Ferreira,[1] An-Sofie Vanherwegen,[1] Guy Eelen,[2,3] Ana Carolina Fierro Gutiérrez,[4] Leentje Van Lommel,[5] Kathleen Marchal,[4,6,7] Lieve Verlinden,[1] Annemieke Verstuyf,[1] Tatiane Nogueira,[8] Maria Georgiadou,[2,3] Frans Schuit,[5] Décio L. Eizirik,[8] Conny Gysemans,[1] Peter Carmeliet,[2,3] Lut Overbergh,[1,9,*] and Chantal Mathieu[1,9]

[1]Laboratory of Clinical and Experimental Endocrinology, Department of Clinical and Experimental Medicine, KU Leuven, Leuven 3000, Belgium
[2]Laboratory of Angiogenesis and Neurovascular Link, Vesalius Research Center, VIB, Leuven 3000, Belgium
[3]Laboratory of Angiogenesis and Neurovascular Link, Vesalius Research Center, VIB, Department of Oncology, KU Leuven, Leuven 3000, Belgium
[4]Department of Microbial and Molecular Systems, KU Leuven, Leuven 3000, Belgium
[5]Gene Expression Unit, Department of Cellular and Molecular Medicine, KU Leuven, Leuven 3000, Belgium
[6]Department of Plant Biotechnology and Bioinformatics, Ghent University, Ghent 9000, Belgium
[7]Department of Information Technology, IMinds, Ghent University, Ghent 9000, Belgium
[8]Laboratory of Experimental Medicine, Free University of Brussels, Brussels 1050, Belgium
[9]Co-senior author
*Correspondence: lut.overbergh@med.kuleuven.be
http://dx.doi.org/10.1016/j.celrep.2015.01.013

SUMMARY

Metabolic switches in various immune cell subsets enforce phenotype and function. In the present study, we demonstrate that the active form of vitamin D, 1,25-dihydroxyvitamin D_3 ($1,25(OH)_2D_3$), induces human monocyte-derived tolerogenic dendritic cells (DC) by metabolic reprogramming. Microarray analysis demonstrated that $1,25(OH)_2D_3$ upregulated several genes directly related to glucose metabolism, tricarboxylic acid cycle (TCA), and oxidative phosphorylation (OXPHOS). Although OXPHOS was promoted by $1,25(OH)_2D_3$, hypoxia did not change the tolerogenic function of $1,25(OH)_2D_3$-treated DCs. Instead, glucose availability and glycolysis, controlled by the PI3K/Akt/mTOR pathway, dictate the induction and maintenance of the $1,25(OH)_2D_3$-conditioned tolerogenic DC phenotype and function. This metabolic reprogramming is unique for $1,25(OH)_2D_3$, because the tolerogenic DC phenotype induced by other immune modulators did not depend on similar metabolic changes. We put forward that these metabolic insights in tolerogenic DC biology can be used to advance DC-based immunotherapies, influencing DC longevity and their resistance to environmental metabolic stress.

INTRODUCTION

Besides the well-established function of the active vitamin D metabolite as central regulator of mineral and bone homeostasis, 1,25-dihydroxyvitamin D_3 ($1,25[OH]_2D_3$) has been rediscovered as a major modulator of the immune system, playing a potential physiological role in the regulation of innate and adaptive immune responses. Although affecting the immune system at different levels, the main target of vitamin D in a mixed immune population is the dendritic cell (DC). In these cells, $1,25(OH)_2D_3$ can generate in vitro a stable maturation-resistant tolerogenic phenotype, with low expression of HLA-DR, low expression of costimulatory molecules (e.g., CD80, CD86), and increased interleukin 10 (IL-10)/IL-12p70 ratios that are maintained even after removal of the compound (van Halteren et al., 2002). Importantly, introduction of an antigen in parallel with $1,25(OH)_2D_3$ can induce antigen-specific tolerogenic DCs (tolDCs) (Unger et al., 2009) with the capacity to induce infectious tolerance, changing the behavior of other proinflammatory mature DCs through the induction of antigen-specific regulatory T cells (Tregs), and causing the perpetuation of the tolerogenic response (Kleijwegt et al., 2011). In addition, $1,25(OH)_2D_3$-conditioned fully differentiated DCs ($1,25D_3$-DCs) lose their ability to activate autoreactive T cells, stimulating instead the generation of Tregs (Ferreira et al., 2014; Unger et al., 2009; van Halteren et al., 2002, 2004). Reintroduction of such $1,25D_3$-DCs in vivo leads to immune modulation (Ferreira et al., 2014), which represents a reliable strategy for the promotion or restoration of antigen-specific tolerance through vaccination strategies, for example, in type 1 diabetes patients. Although these immunomodulatory effects of $1,25(OH)_2D_3$ on DC phenotype and function are well delineated, the intracellular and molecular mechanisms leading to these tolerogenic properties remain largely unknown.

Recently, metabolic regulation has emerged as an essential mechanism to control the function, growth, proliferation, and survival of various immune cell subsets, an area of research referred to as "immunometabolism" (Williams et al., 2013). Thus,

the crosstalk between different immune signals and the metabolic status of T cells and macrophages, in particular, direct key immune cell-fate decisions (Michalek et al., 2011; Vats et al., 2006; Zeng et al., 2013). Moreover, metabolic changes occur within minutes in murine DCs upon toll-like receptor (TLR)-induced maturation and commit DCs to switch from oxidative phosphorylation (OXPHOS) to glycolysis. TANK-binding kinase 1 (TKB1), IκB kinase-ε (IKKε), and Akt signaling were shown to be essential for the TLR-induced transition to aerobic glycolysis by promoting the association of the glycolytic enzyme hexokinase-2 (HK2) with mitochondria. This metabolic pathway seems crucial for sustaining cell survival and function (Everts et al., 2012, 2014; Krawczyk et al., 2010).

Building on our previous findings obtained by proteomic analysis suggesting that $1,25(OH)_2D_3$ has a major impact on metabolic proteins in fully differentiated DCs (Ferreira et al., 2012), we have now studied the early intracellular pathways activated by $1,25(OH)_2D_3$ in these cells. This was done by a combination of transcriptome analysis and functional studies of the identified pathways, with a major focus on metabolic changes. The data obtained indicate that $1,25(OH)_2D_3$ initiates an early transcriptional reprogramming of metabolic pathways in not yet fully differentiated human DCs (differentiating monocytes, dMo) that favors OXPHOS, which is accompanied by increased aerobic glycolysis. Furthermore, $1,25D_3$-DCs, but not tolDCs generated by other biological and pharmacological agents, rely on glucose availability and usage, as well as on the PI3K/Akt/mTOR pathway, for the induction and maintenance of their tolerogenic phenotype. The present findings show that $1,25(OH)_2D_3$ affects the phenotype and behavior of DCs through its impact on cellular metabolic pathways, driving both OXPHOS and glycolysis in a way that is unique to this compound.

RESULTS

Tolerogenic DCs Generated by $1,25(OH)_2D_3$ Present an Early and Transcriptionally Mediated Metabolic Reprogramming

In order to elucidate the molecular mechanisms underlying the tolerogenic properties of $1,25D_3$-DCs, we performed microarray analysis of human dMo at 4 and 24 hr after addition of differentiation media (e.g., IL-4 and granulocyte macrophage colony-stimulating factor [GM-CSF]) and $1,25(OH)_2D_3$ (10^{-8} M) (Figure S1). These early time points were chosen based on the observation that a single dose of $1,25(OH)_2D_3$ to dMo at the start of the in vitro DC culture was sufficient to generate the tolerogenic profile, because we observed a similar decrease in CD80/HLA-DR and an increase in CD14 surface expression, when compared to DCs exposed to two administrations of $1,25(OH)_2D_3$ (Széles et al., 2009; Figure S2). Four hours of treatment with $1,25(OH)_2D_3$ induced the differential expression of 100 genes, compared to controls (1.3-fold change; adjusted $p < 0.01$) (Figure S3A, left panel). Among these are known $1,25(OH)_2D_3$-regulated genes, such as *CYP24A1*, *CCL22*, *CD14*, *CD200*, and *CA2* (Figure S3A, right panel), confirming the early responsiveness of this cell type to $1,25(OH)_2D_3$ (Figure S3B). Comparing the transcriptomes of $1,25(OH)_2D_3$-conditioned and vehicle-treated samples after 24 hr of in vitro culture revealed the differential expression of 1,558 genes. Only 68 of these were modified by the hormone at both time points (Figure S3A, left panel).

Classification of the genes affected after 24 hr of $1,25(OH)_2D_3$ treatment by Gene Ontology (GO) revealed that four out of the top nine preferentially affected biological processes corresponded to metabolism-related pathways, namely, tricarboxylic acid cycle (TCA), OXPHOS, respiratory electron transport chain (ETC), and mitochondrial electron transport, NADH to ubiquinone (all $p < 0.05$ compared to vehicle-treated dMo) (Table S1). Similarly, grouping this set of genes according to their function in different biological pathways using Reactome, seven out of the top 12 affected pathways were related to metabolic processes (Table S2).

To identify candidate pathways preferentially affected by $1,25(OH)_2D_3$ treatment in human dMo, we subjected the same set of genes to ingenuity pathway analysis (IPA). This revealed that $1,25(OH)_2D_3$ treatment induced several highly ranked canonical pathways related to oxidative metabolism and glycolytic control, namely, OXPHOS, mitochondrial dysfunction, the TCA cycle, and PI3K signaling (Figure S3C; Table S3). The majority of the genes related to the TCA cycle, and OXPHOS were upregulated after $1,25(OH)_2D_3$ treatment compared to control condition (Figure S4). Similarly, key metabolic genes involved in glucose uptake and glycolytic commitment/control were upregulated by the hormone, whereas mRNA expression of inhibitory molecules, such as pyruvate dehydrogenase kinase isozyme 4 (*PDK4*), were downregulated (Figure S4). Taken, together these results indicate that $1,25(OH)_2D_3$ induces an early metabolic reprogramming in human dMo, which is characterized by the transcriptional upregulation of several genes directly related to the TCA cycle, OXPHOS, and glucose metabolism.

Tolerogenic DCs Induced by $1,25(OH)_2D_3$ Have an Increased Oxidative Metabolism

The main transcripts related to glucose metabolism, the TCA cycle, and OXPHOS identified by the microarray analysis are shown in Figures 1A and 2A. qRT-PCR was used to validate the observed changes in some of these key genes, confirming an upregulated mRNA expression 24 hr after addition of $1,25(OH)_2D_3$ of glucose receptor 3 (*GLUT3*), the glucose receptor of white blood cells; hexokinase 3 (*HK3*), the enzyme responsible for committing glucose to the glycolytic pathway; 6-phosphofructo-2-kinase/fructose-2,6-biphosphatase 4 (*PFKFB4*), which regulates phosphofructokinase and functions as regulatory enzyme of glycolysis, besides being a putative direct target of $1,25(OH)_2D_3$ in THP-1 cells (Heikkinen et al., 2011); pyruvate dehydrogenase alpha 1 (*PDHA1*), one of the subunits of the pyruvate dehydrogenase complex and a central link between glycolysis and the TCA cycle; ATP synthase subunit alpha 1 (*ATP5A1*), which catalyzes ATP synthesis during OXPHOS; and lactate dehydrogenase A (*LDHA*), which produces lactate from pyruvate during glycolysis (Figure 1B).

Interestingly, *AMPK*, a master regulator of ATP production through fatty acid (FA) oxidation, was upregulated 24 hr after addition of $1,25(OH)_2D_3$ to the human dMo cultures (Figure 1C). The total protein levels of ACC, a direct AMPK target, were also induced in human dMo conditioned by $1,25(OH)_2D_3$ as early as 48 hr after addition of the hormone, whereas its phosphorylation

levels were slightly upregulated in the same samples, as compared to controls (Figure 1D).

Because OXPHOS is often linked to the induction of a tolerogenic phenotype of different immune cell subsets (Michalek et al., 2011; Vats et al., 2006), we performed functional assays to further investigate whether human 1,25D_3-DCs showed features pointing to an induced OXPHOS metabolism. Treatment with the hormone increased the intracellular ATP content and ROS production, as compared to controls, throughout the complete culture period (Figure 1E). Furthermore, the mitochondrial membrane potential and total mitochondrial mass were increased by 1,25$(OH)_2D_3$ in human dMo (Figure 1F). Finally, human 1,25D_3-DCs showed a clear trend for higher basal oxygen consumption rate (OCR) (Figure 1G) and a significantly increased glucose oxidation (Figure 1H), as compared to controls. Interestingly, FA and glutamine (Q) oxidation rates were not significantly changed in human 1,25D_3-DCs (Figure 1H). Together, these data support the view that human tolDCs obtained in vitro in the presence of 1,25$(OH)_2D_3$ have an increased OXPHOS profile with glucose as main oxidative fuel, a process that is maintained throughout the differentiation/maturation culture period.

1,25$(OH)_2D_3$-Modulated Tolerogenic DCs Perform Increased Glycolysis in the Presence of Oxygen

The microarray data described above suggested that human 1,25D_3-DCs not only have increased oxidation, but also perform increased glycolysis. This is clear from the induced expression of both *PFKFB4* and *LDHA* (Figure 1B), as well as several other enzymes directly involved in this pathway in human dMo conditioned by 1,25$(OH)_2D_3$ (Figure 2A). We further evaluated whether this increased glycolytic transcriptional profile was paralleled by an altered functional profile. The basal extracellular acidification rate (ECAR), which indicates pH changes that may occur due to lactate production, was increased in human 1,25D_3-DCs as compared to vehicle-treated control DCs (Ctr-DCs) (Figure 2B). In line with this, 1,25D_3-DCs secreted increasing levels of lactate, as evidenced by an accumulation of the media lactate content throughout the complete in vitro culture period. This was accompanied by increased glucose uptake rates and a gradual decrease in the media glucose content, as compared to controls (Figure 2C). Finally, human 1,25D_3-DCs clearly present an induction in their glycolytic rate, as compared to controls (Figure 2D). Taken together, these data show that human tolDCs obtained in vitro in the presence of 1,25$(OH)_2D_3$ use glucose as metabolic fuel in both OXPHOS and aerobic glycolysis.

Glucose Availability Plays an Essential Role in Inducing and Maintaining the Tolerogenic Phenotype and Function of 1,25$(OH)_2D_3$-Treated DCs

Next, we investigated the impact of glucose availability in inducing and maintaining the 1,25D_3-DC phenotype in vitro. As expected, human 1,25D_3-DCs obtained at 10 mM glucose presented a typical tolerogenic cell-surface phenotype, with lower expression levels of CD80, CD86, and HLA-DR and increased IL-10/IL-12p70 ratios as compared to Ctr-DCs (Figure 3A). When subjecting human dMo to a glucose-limiting condition, i.e., 1 mM, the 1,25D_3-DC phenotype was completely prevented, as evidenced by unaltered CD86 and HLA-DR expression and increased CD80 levels as compared to controls, without impacting cell survival (Figures 3A and S5A). In line with this, lower IL-10/IL-12p70 ratios were detected during glucose deprivation (versus similar culture conditions at 10 mM glucose availability, see Figure 3A). The prevention of the tolerogenic phenotype induced by 1,25$(OH)_2D_3$ in human DCs was confirmed after evaluation of T cell proliferation and interferon γ (IFN-γ) secretion into the culture supernatants, because 1,25D_3-DCs obtained in the presence of 1 mM glucose partially restored their ability to promote T cell proliferation. This was especially clear for $CD4^+$ T cells and was followed by a full impairment in IFN-γ secretion into the coculture supernatants, as compared to their respective controls (Figure 3A). Interestingly, adjusting glucose levels to 10 mM every day during the in vitro culture period neither improved the tolerogenic surface phenotype of 1,25D_3-DCs (Figure S5B), nor altered the rate of glucose consumption and lactate production (Figures S5C–S5F). These experiments allowed us to conclude that sufficiently available glucose in culture media, especially in the beginning of the differentiation period, plays an essential role in the induction and maintenance of the tolerogenic phenotype of human 1,25D_3-DCs.

Next, we attempted to generate in vitro human 1,25D_3-DCs in hypoxic conditions (0.2% available oxygen) and thus under limiting OXPHOS rates. These conditions partially impaired the tolerogenic effects of 1,25$(OH)_2D_3$ on the surface expression of CD86 and HLA-DR of human DCs. These alterations did not change the ability of 1,25D_3-DCs to hamper T cell function in vitro, even though IFN-γ secretion was affected, indicating that oxygen availability did not play an essential role in inducing and maintaining the tolerogenic function of human 1,25D_3-DCs. Limiting the availability of oxygen did however impair 1,25D_3-DC survival (Figures 3B and S5G).

Glycolysis, but Not Glucose and FA Oxidation, Is Essential for the Induction and Maintenance of the Tolerogenic Phenotype of 1,25$(OH)_2D_3$-Modulated DCs

Because glucose uptake, oxidation, and especially glycolysis was clearly induced in human 1,25D_3-DCs, we tried to obtain 1,25D_3-DCs in the presence of 2-deoxy-D-glucose (2-DG), a glucose analog that is phosphorylated by HK to 2-DG-phosphate, which cannot be further metabolized. Accumulation of 2-DG-phosphate inhibits glycolysis causing ATP depletion. Previous studies have used low doses of 2-DG to address the influence of glycolysis in directing the cell fate of $CD4^+$ Th17 cells versus $Foxp3^+$ Tregs (Michalek et al., 2011; Shi et al., 2011). Addition of 5 mM 2-DG to human iDC conditioned with 1,25$(OH)_2D_3$ decreased the accumulation of lactate in the media (as compared to 1,25D_3-DCs obtained in 10 mM glucose media, Figure 4A), prevented the downregulation of HLA-DR, CD80 and CD86, in addition to decreasing the IL-10/IL-12 ratios (as compared to 1,25D_3-DCs) (Figure 4B). The inhibition of the tolerogenic phenotype of the human 1,25D_3-DCs was confirmed after evaluation of T cell proliferation, because 1,25D_3-DCs obtained in the presence of 5 mM 2-DG partially restored their ability to promote T cell function, especially $CD4^+$ T cell proliferation (Figure 4B).

We next exposed human 1,25D_3-DCs to dichloroacetate (DCA) (a PDK inhibitor, which pushes glucose-derived pyruvate

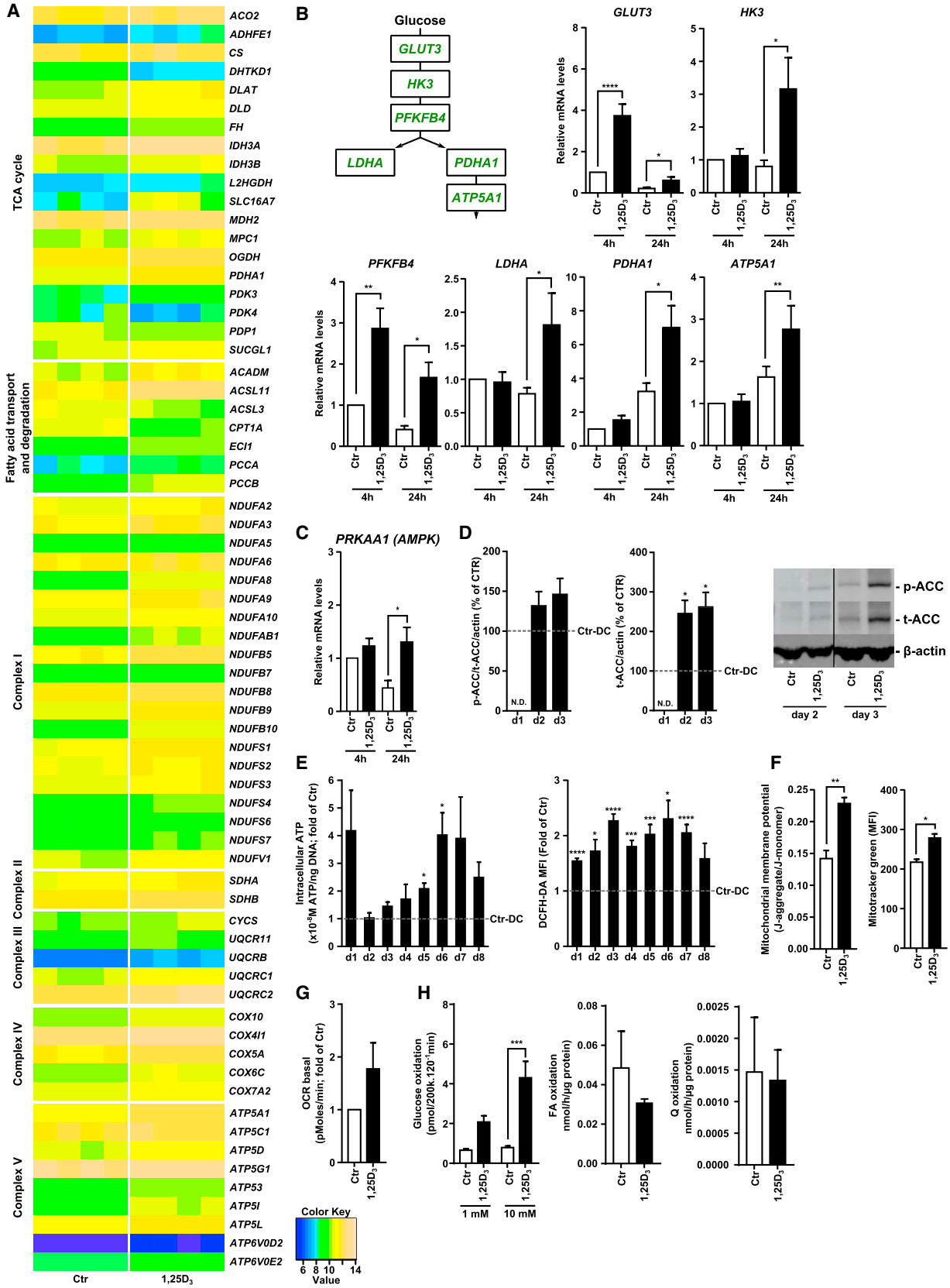

(legend on next page)

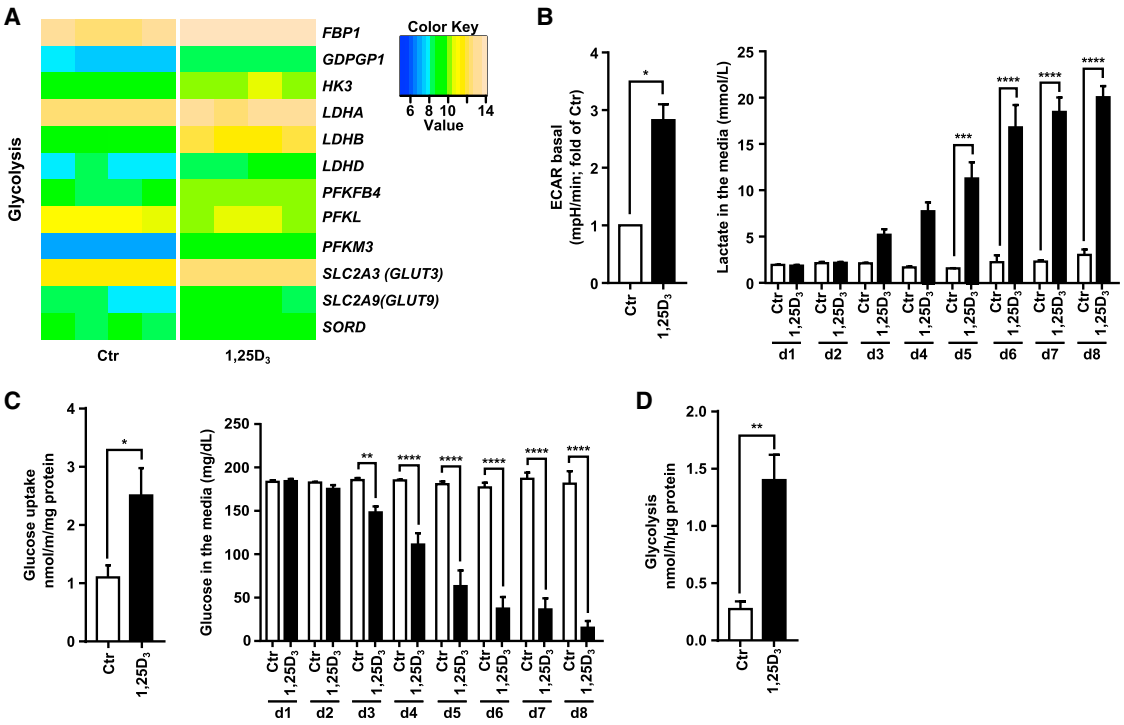

Figure 2. 1,25(OH)$_2$D$_3$-Modulated DCs Have Increased Glycolytic Metabolism

(A) Heatmap generated from microarray data reflecting differentially expressed genes corresponding to proteins included in the glycolytic branch of the metabolic pathway.

(B) Basal ECAR of Ctr- or 1,25D$_3$-DCs measured using Seahorse technology (n = 3; *p < 0.05); media lactate content of Ctr- (white bars) or 1,25D$_3$-DCs (black bars), measured daily during the complete differentiation and maturation period from monocytes (n = 3–7; **p < 0.01, ***p < 0.001, ****p < 0.0001).

(C) Glucose uptake of Ctr- (white bars) or 1,25D$_3$-DCs (black bars) (n = 4; *p < 0.05 as compared to controls); media glucose content of Ctr- (white bars) or 1,25D$_3$-DCs (black bars), measured daily during the complete differentiation and maturation period from monocytes (n = 3–7; **p < 0.01, ***p < 0.001, ****p < 0.0001).

(D) Glycolytic flux of Ctr- (white bars) or 1,25D$_3$-DCs (black bars) (n = 3–4; p < 0.01). Values depicted in the bar graphs represent average levels ± SEM from either metabolite in the supernatants of Ctr- (white bars) or 1,25D$_3$-DC (black bars) cultures.

into the mitochondria for further metabolism and thus induces metabolic switch from glycolysis to mitochondrial respiration; Figure 4A) to investigate whether the fate of pyruvate is important in the induction and maintenance of a tolerogenic profile in 1,25D$_3$-DCs. Also here, in spite of a reversal in the expression of CD86 on the DC cell surface, neither major changes in other phenotypic markers nor on the ability of DCs to stimulate T cell proliferation and IFN-γ production were observed (Figure 4C). Similarly, exposure of human 1,25D$_3$-DCs to etomoxir, an inhibitor that prevents FA transport into the mitochondria and thus

Figure 1. 1,25(OH)$_2$D$_3$-Modulated DCs Have an Upregulated Oxidative Metabolism

(A) Heatmaps generated from the microarray data reflecting differentially expressed genes corresponding to proteins included in the oxidative branch of the metabolic pathway.

(B) Confirmation of differential mRNA expression of *GLUT3*, *HK3*, *PFKFB4*, *PDHA1*, *ATP5A1*, and *LDHA* by qRT-PCR in Ctr- (white bars) or 1,25D$_3$-dMo (black bars) (n = 5–12; *p < 0.05, **p < 0.01).

(C) Confirmation of differential expression of the relative mRNA levels of *PRKAA1* (*AMPK*) was performed by qRT-PCR of Ctr- (white bars) or 1,25D$_3$-dMo (black bars) (n = 6; *p < 0.05).

(D) Total protein lysates of Ctr- and 1,25D$_3$-dMo samples prepared at days 1–3 after addition of 1,25(OH)$_2$D$_3$ and differentiation media. Protein levels of phosphorylated and total ACC (normalized to β-actin) were determined by western blot; the bar graphs represent the average ratio ± SEM of the percentage induction/inhibition of the analyzed proteins in Ctr- versus 1,25D$_3$-dMo by western blot (n = 3; *p < 0.05; N.D., not detectable).

(E) Intracellular ATP content (left) and ROS production (right) in Ctr- or 1,25D$_3$-dMos and in fully differentiated Ctr- or 1,25D$_3$-DCs. Bar graphs illustrate the fold change in the production of either metabolite in 1,25(OH)$_2$D$_3$-modulated cells, as compared to controls (n = 4; *p < 0.05, ***p < 0.001, ****p < 0.0001).

(F) Mitochondrial membrane potential measured after JC-1 staining of ethanol- (white bar) or 1,25(OH)$_2$D$_3$-modulated iDCs (black bar); mitochondrial mass determined after staining with Mitotracker green and FACS analysis of Ctr- or 1,25D$_3$-iDCs (n = 3; *p < 0.05).

(G) Basal OCR of Ctr- or 1,25D$_3$-DCs measured by Seahorse technology (n = 3).

(H) Glucose (1 and 10 mM available glucose), FA, and Q oxidation rates of Ctr- (white bars) or 1,25D$_3$-DCs (black bars) (n = 3–4; ***p < 0.001 as compared to controls).

In (A)–(H), values depicted in the bar graphs represent average ± SEM from the measured parameters in Ctr- (white bars) or 1,25D$_3$-DCs (black bars).

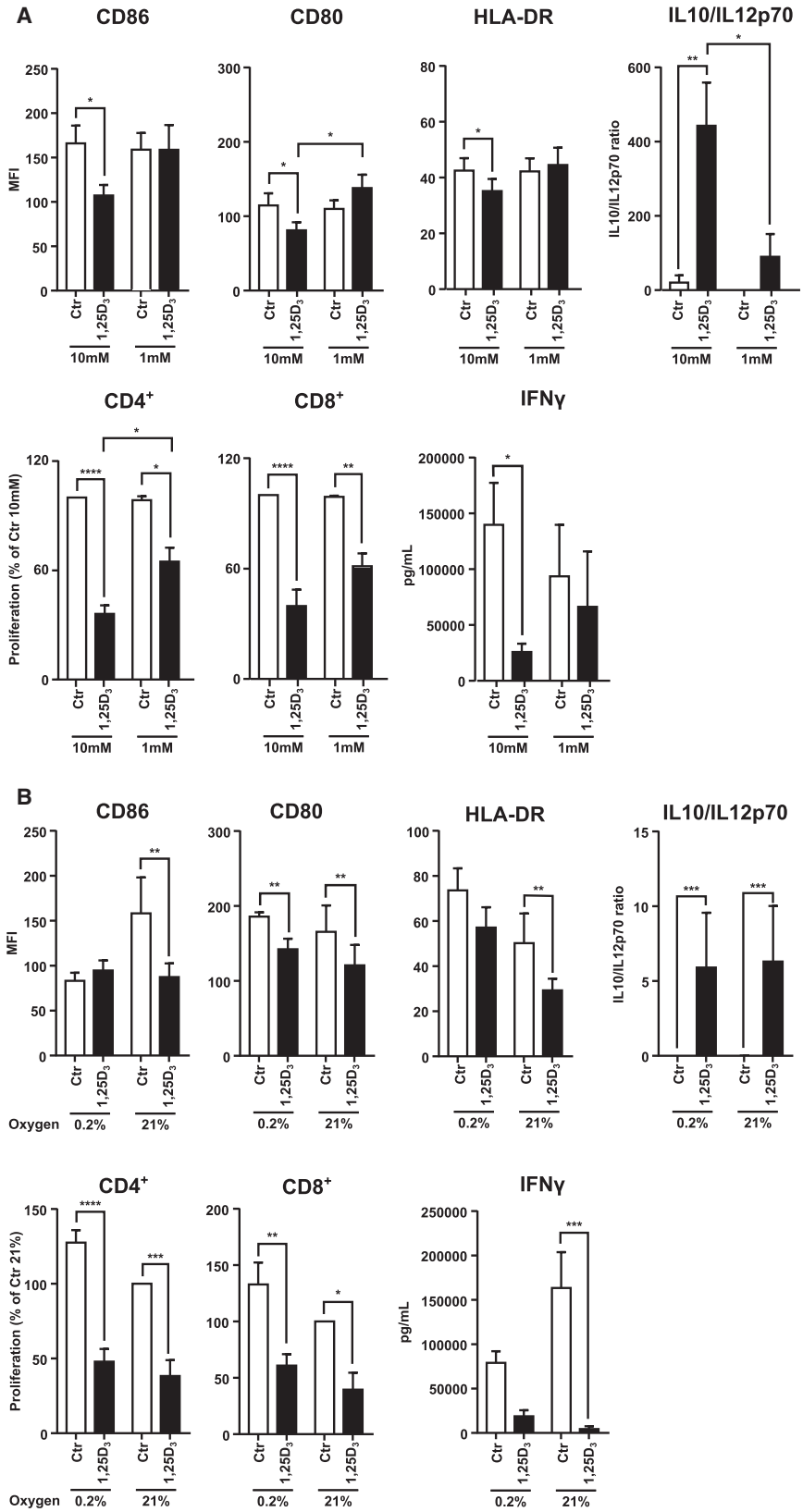

Figure 3. 1,25(OH)$_2$D$_3$-Modulated DCs Depend on Glucose Availability to Maintain Their Tolerogenic Phenotype

Human Ctr- and 1,25D$_3$-DCs were obtained in vitro in the presence of (A) 1–10 mM glucose or (B) 0.2%–21% O_2. Ctr- (white bars) or 1,25D$_3$-DCs (black bars). Cells were analyzed by FACS for the detection of surface expression of different markers (CD86, CD80, HLA-DR) (n = 4–10; *p < 0.05, **p < 0.01). Values depicted in the bar graphs represent the levels of the mean fluorescence intensity (MFI) ±SEM from cell-surface markers. ELISA was used to analyze the release of the cytokines IL-10 and IL-12p70 to the culture supernatants, and the values were then expressed as the ratio IL-10/IL-12p70 (n = 4–10, *p < 0.05, **p < 0.01, ***p < 0.001). Proliferation of labeled T cells was analyzed after 4 days in coculture by means of eFluor670 cell proliferation dye dilution. The results were expressed as percentage ±SEM of proliferation inhibition of CD4$^+$ (left) or CD8$^+$ (right) T cells, with proliferation in the presence of Ctr-DCs set as 100% (n = 4; *p < 0.05, **p < 0.01, ***p < 0.001, ****p < 0.0001); IFN-γ levels were measured in culture supernatants of the DC:T cell cocultures (n = 4, ***p < 0.001).

reduces FA oxidation rates (Figure 4A), did not alter the tolerogenic phenotype and function of 1,25D_3-DCs (Figure 4D). Altogether, these results suggest that glycolysis, but not glucose or FA oxidation, influences the tolerogenic phenotype onset in 1,25D_3-DCs.

The PI3K/Akt/mTOR Pathway Is Essential for 1,25$(OH)_2D_3$-Modulated DCs to Maintain Their Tolerogenic Phenotype In Vitro

The findings described above suggest that human 1,25D_3-DCs rely on glucose availability and aerobic glycolysis to maintain their tolerogenic properties. Signaling through the PI3K/Akt/mTOR pathway is central to the regulation of glycolytic metabolism (Locasale and Cantley, 2011; Shaw and Cantley, 2006), and, consistent with this, PI3K and Akt play an essential role in sustained commitment to glycolysis in activated DCs (Krawczyk et al., 2010). Because this pathway also controls the expression of *C-MYC*, a transcription factor that plays an essential role in facilitating glycolysis, and of different proteins involved in glucose uptake and glycolytic enzymes (Figure 5A), we further investigated its impact on the induction of human 1,25D_3-DCs. *PIK3CG*, one of the catalytic subunits of the PI3K complex, was found upregulated at the mRNA level, as evidenced both by microarray analysis and by qRT-PCR (versus Ctr-DCs) (Figure 5B). In addition, expression of *C-MYC* was upregulated in 1,25D_3-DCs, as compared to controls (Figure 5B). Furthermore, although mRNA expression of *AKT* was downregulated in 1,25D_3-DCs (Figure 5B), the levels of p-Akt were maintained constant in 1,25D_3-DCs, but decreased in Ctr-DCs. This resulted in a 6.03 ± 1.82-fold upregulation of activated Akt in treated cells, as compared to controls, 72 hr after exposure of dMo to 1,25$(OH)_2D_3$ (Figures 5C and 5D). The functional activation of Akt was confirmed by the increased phosphorylation of two of its downstream targets, namely, mTOR and GSK-3β, 48 and 72 hr after exposure of dMo to 1,25$(OH)_2D_3$, respectively (Figures 5C and 5D).

We next explored the role of the PI3K/Akt/mTOR pathway on the phenotype and function of human 1,25D_3-DCs by making use of different small molecule inhibitors (Figure 6A). Inhibition of the PI3K/Akt/mTOR pathway by LY294002, a specific PI3K-inhibitor, or by rapamycin (RAPA), a natural mTOR inhibitor, completely normalized the decrease of glucose levels previously observed in 1,25D_3-DC cultures (Figure 6B). Similar data were obtained when normalizing the glucose levels to the amount of living cells in the culture (data not shown). This was paralleled by normalization of the expression of CD86 and HLA-DR in LY294002-1,25D_3-DCs (versus vehicle-1,25D_3-DCs), as well as a trend for increased CD80 expression (Figure 6B). In line with these findings, LY294002-1,25D_3-DCs had decreased IL-10/IL-12p70 ratios, when compared to vehicle-1,25D_3-DCs (Figure 6A), demonstrating a full phenotype prevention in LY294002-1,25D_3-DCs. Addition of RAPA to the DC cultures induced, to some extent, similar effects as LY294002 with restored CD86 expression and decreased IL-10/IL-12p70 ratios, as compared to respective controls (Figure 6B). Of interest, 1,25D_3-DCs were largely dependent on the PI3K/Akt/mTOR pathway for survival, as shown by the increased cell death levels in vitro when 1,25D_3-DCs were cultured in the presence of either LY294002 or RAPA (versus vehicle-1,25D_3-DCs) (Figure S6A).

Differentiation of DCs in the presence of AICAR, an AMPK-activator, produced similar, although less clear, surface marker expression changes in 1,25D_3-DCs. This was paralleled by a similar restoration of media glucose levels (versus vehicle-1,25D_3-DCs) (Figure 6B). Of note, AICAR-1,25D_3-DCs secreted increased IL-10/IL-12p70 ratios (Figure 6B). Together, these data clearly indicate that 1,25$(OH)_2D_3$ relies on the PI3K/Akt/mTOR axis to induce and maintain a stable tolerogenic phenotype in human-monocyte-derived 1,25D_3-DCs.

Finally, we investigated whether other immunomodulatory compounds (dexamethasone [DEX], ITF2357 [a histone deacetylase inhibitor], IL-10, and RAPA) also rely on PI3K/Akt/mTOR to induce tolerogenicity in human-monocyte-derived DCs. First, we observed that none of these compounds induced the characteristic decrease in media glucose levels previously observed in 1,25D_3-DC cultures (Figure 6D). Furthermore, none of the surface marker molecules investigated showed altered expression when the PI3K/Akt/mTOR pathway was blocked using LY294002 (Figure 6D) or AICAR (Figure S5B). These findings suggest a different mechanism of action for 1,25$(OH)_2D_3$, as compared to the other tolerance-inducing agents, in the induction of tolDCs, with glycolysis and the PI3K/Akt/mTOR pathway being uniquely required by 1,25$(OH)_2D_3$. The other types of tolDCs do, however, seem to rely on the PI3K pathway for survival (Figure S6C).

Inhibition of the PI3K/Akt/mTOR Pathway Reverses the Tolerogenic Function of 1,25$(OH)_2D_3$-Modulated DCs

To elucidate the functional impact of the PI3K pathway on the induction of 1,25D_3-DCs, we investigated whether their T cell activation capacity could be restored by directly interfering with this pathway using LY294002 or RAPA. As expected, 1,25D_3-DCs decreased $CD4^+$ and $CD8^+$ T cell proliferation and decreased IFN-γ production, as compared to Ctr-DCs. Addition of LY294002 or RAPA to 1,25D_3-DCs prevented the function of these tolDCs, as shown by a partial restoration of T cell proliferation when compared to vehicle-1,25D_3-DCs; this was particularly evident in the case of $CD4^+$ T cells (Figure 7A). In agreement with the surface phenotype expression of tolDCs obtained in the presence of different tolerogenic compounds and LY294002, this functional impairment of the tolDC phenotype was only induced in LY294002-1,25D_3-DCs and not with the other tolerogenic agents (data not shown). The increased T cell proliferative response was paralleled by an increased production of IFN-γ into the supernatant of the cocultures (Figure 7B), indicating that the PI3K/Akt/mTOR pathway is essential for human 1,25D_3-DCs to maintain not only their tolerogenic phenotype, but also their immunoregulatory function.

DISCUSSION

Immune cells do not only depend on nutrients for survival, but oxygen and energy source also determine to a large extent their fate and functional status. Several environmental and other clues influence the metabolic switches in these cells (Delmastro-Greenwood and Piganelli, 2013). Most of the phenomena accompanying immunological responses involve changes

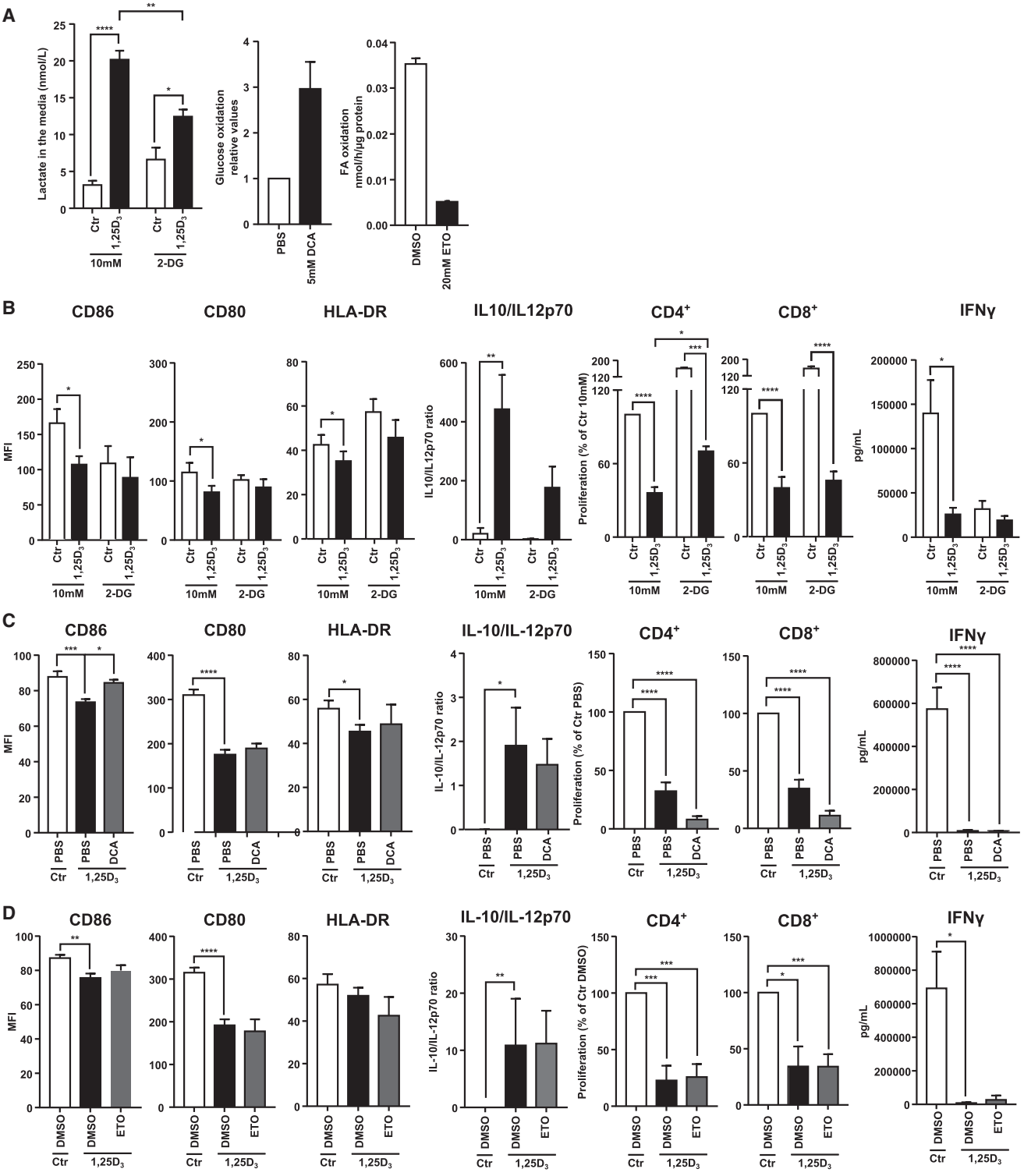

Figure 4. 1,25(OH)$_2$D$_3$-Modulated DCs Depend on Glycolysis, but Not on Glucose or FA Oxidation, to Induce and Maintain Their Tolerogenic Phenotype

(A) The concentrations of inhibitors used were tested in 1,25D$_3$-DCs (2-DG and DCA) or Ctr-DCs (etomoxir), and cells were further evaluated for glucose and FA oxidation using radiolabeled metabolites, as well as for the secretion of lactate into de media.

(B) Human Ctr- and 1,25D$_3$-DCs were obtained in vitro in the presence of 5 mM 2-DG or 10 mM glucose. Ctr- (white bars) or 1,25D$_3$-DCs (black bars) were analyzed by FACS for the detection of surface expression of different markers (CD86, CD80, HLA-DR) (n = 4–10; *p < 0.05, **p < 0.01). Values depicted in the bar

(legend continued on next page)

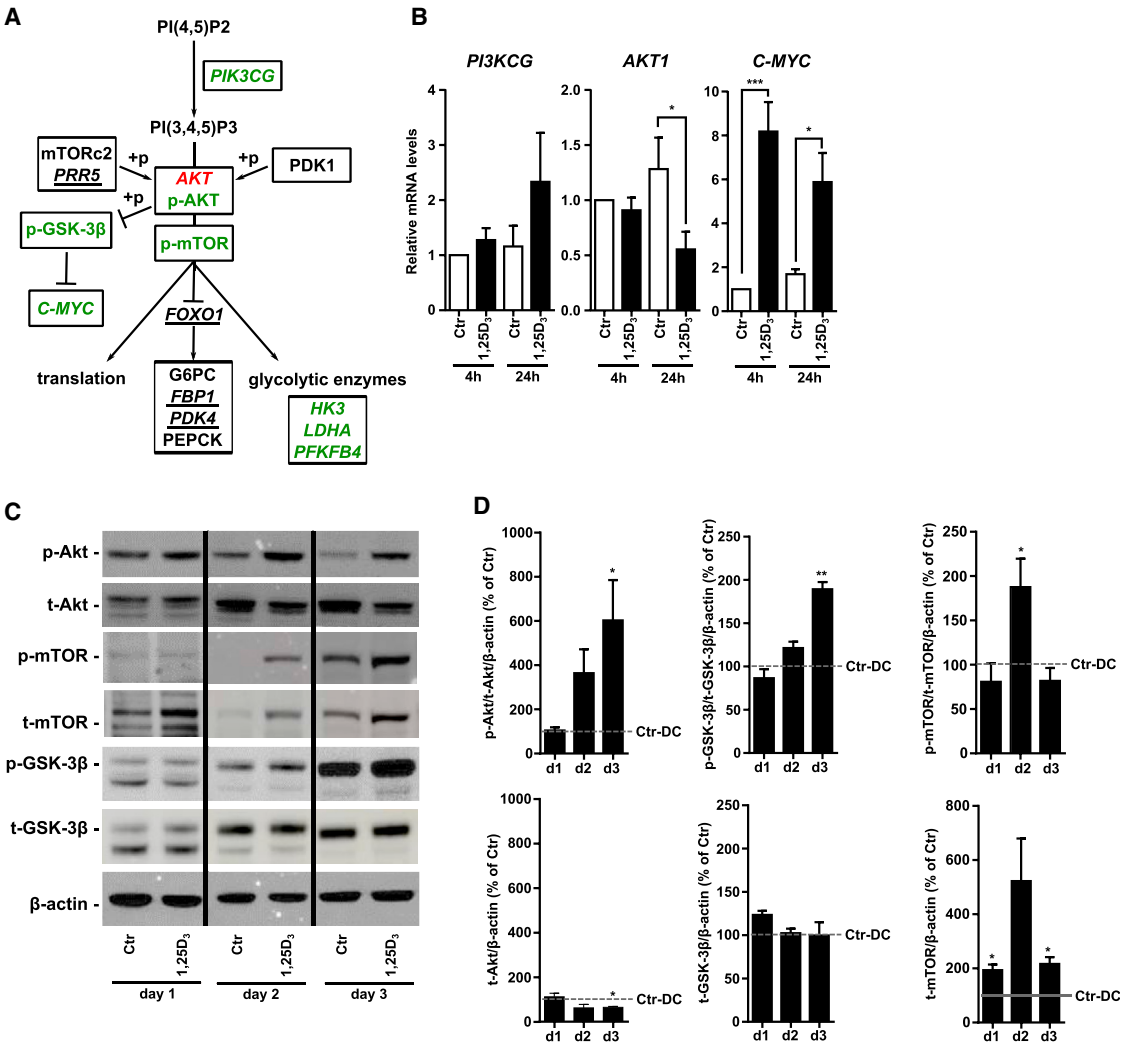

Figure 5. The PI3K/Akt/mTOR Axis Is Activated in 1,25(OH)$_2$D$_3$-Modulated DCs

(A) Schematic representation of the PI3K-Akt-mTOR pathway. Indicated genes were identified as differentially expressed upon 1,25(OH)$_2$D$_3$ treatment after microarray analysis (italic and underlined font, black color), identified after microarray analysis with differential expression confirmed by qRT-PCR (italic font; green color: upregulated genes; red: downregulated gene), or confirmed to be differentially expressed in 1,25D$_3$-DCs (versus Ctr-DCs) at the protein level (green font).

(B) Confirmation of differential expression of *PIK3CG*, *AKT1*, and *C-MYC* by qRT-PCR analysis of Ctr- (white bars) or 1,25D$_3$-DCs samples (n = 5–6; *p < 0.05).

(C) Total protein lysates of Ctr- and 1,25D$_3$-DCs samples prepared at days 1–3 after addition of 1,25(OH)$_2$D$_3$ and differentiation media. Protein levels of phosphorylated and total Akt/GSK-3β/mTOR (normalized to β-actin) were determined by western blot.

(D) The bar graphs represent the average ratio ± SEM of the percentage induction/inhibition of the analyzed proteins in Ctr- versus 1,25D$_3$-DCs by western blot (n = 3; *p < 0.05).

in gene expression that are thermodynamically demanding, requiring fast metabolic adaptations (Delmastro-Greenwood and Piganelli, 2013; Frauwirth and Thompson, 2004; Krauss et al., 2001). Understanding how metabolic transitions are induced and the nature of their role in supporting or directing phenotypic and functional alterations in immune cells during immune-mediated processes may open new paths for drug development (Pearce and Pearce, 2013).

graphs represent the levels of the mean fluorescence intensity (MFI) ±SEM from cell-surface markers. ELISA was used to analyze the release of the cytokines IL-10 and IL-12p70 to the culture supernatants, and the values were then expressed as the ratio IL-10/IL-12p70 (n = 4–10, *p < 0.05, **p < 0.01, ***p < 0.001). Proliferation of labeled T cells was analyzed after 4 days in coculture by means of eFluor670 cell proliferation dye dilution. The results were expressed as percentage ± SEM of proliferation inhibition of CD4$^+$ (left) or CD8$^+$ (right) T cells, with proliferation in the presence of Ctr-DCs set as 100% (n = 4; *p < 0.05, **p < 0.01, ***p < 0.001, ****p < 0.0001); IFN-γ levels were measured in culture supernatants of the DC:T cell cocultures (n = 4, ***p < 0.001).

(C and D) Human DCs were obtained after in vitro treatment with 5 mm DCA (C) or 20 mM etomoxir (D) and analyzed as described in (B) (n = 4, *p < 0.05, **p < 0.01, ***p < 0.001, ****p < 0.0001).

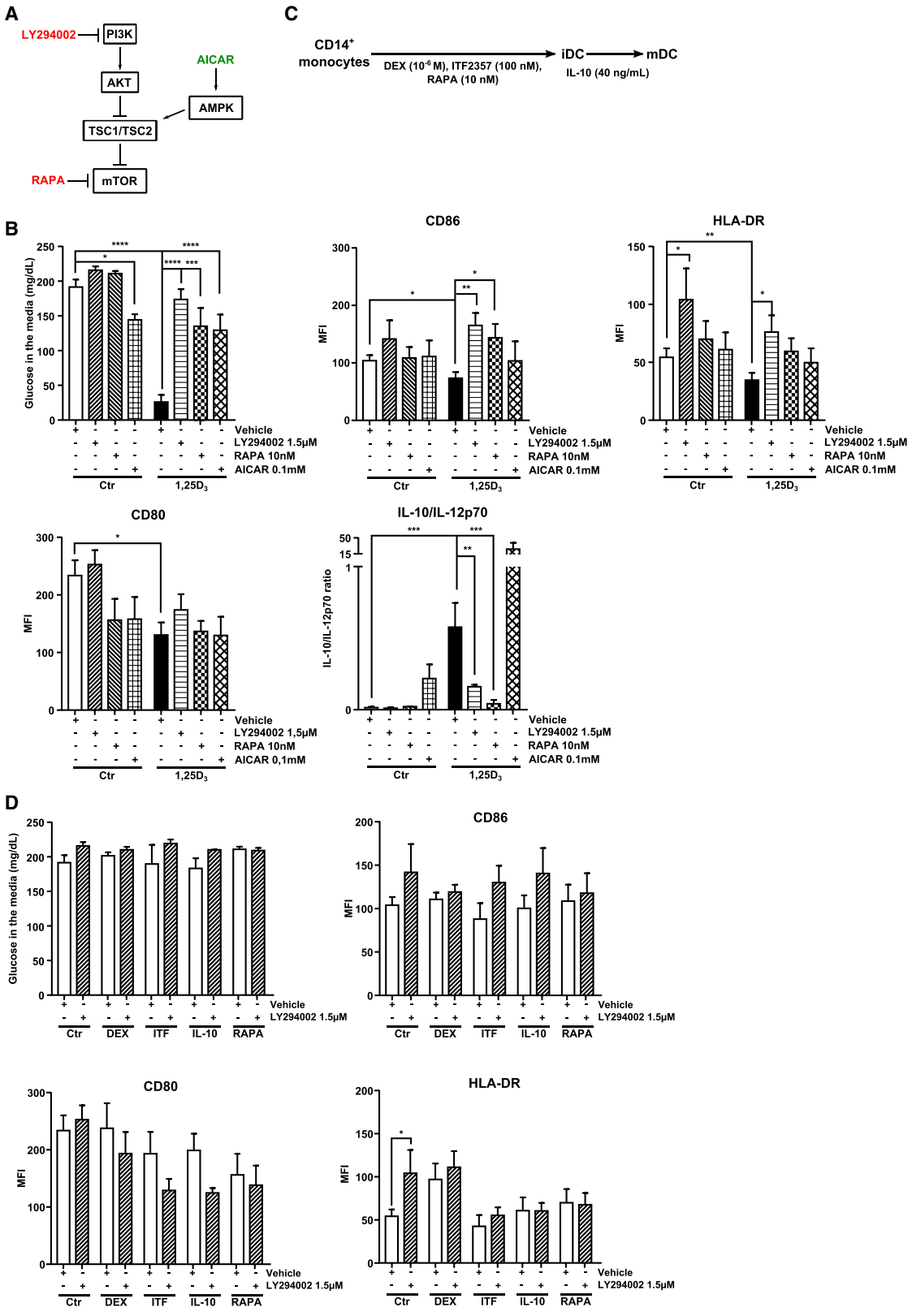

(legend on next page)

The present findings show an early reprogramming of key metabolic pathways by $1,25(OH)_2D_3$, initiated at the mRNA level already at 24 hr after exposure of human dMo to the hormone. This is in agreement with and builds further on our previous findings, where we observed major alterations in metabolic proteins, exclusively in $1,25D_3$-DCs, and not in DEX-modulated DCs (Ferreira et al., 2012). These changes are accompanied by an induced oxidative metabolism in $1,25D_3$-DCs, as evidenced by increased intracellular ATP and ROS production, increased mitochondrial mass and membrane potential, elevated OCR, and induced glucose oxidation rates. Such a switch to OXPHOS linked to a tolerogenic profile is in line with earlier observations indicating that the induction of M2 macrophages in response to IL-4 involves metabolic reprogramming toward FA oxidation and mitochondrial biogenesis, whereas inhibition of oxidative metabolism attenuates the anti-inflammatory program of macrophage activation (Vats et al., 2006). In addition, activated AMPK, which regulates FAO by phosphorylating and inhibiting ACC and consequently stimulating carnitine palmitoyltransferase 1 (CPT1a), the rate-limiting enzyme in FAO, is crucial for Treg development, whereas the Akt/mTOR axis is a negative regulator of de novo Treg differentiation and population expansion (Michalek et al., 2011; Zeng et al., 2013). Moreover, activation of AMPK contributes for the generation of murine tolDCs in the presence of IL-10 (Krawczyk et al., 2010). We have presently observed a parallel induction of OXPHOS and aerobic glycolysis by $1,25(OH)_2D_3$, with an essential role for the availability of glucose in the environment for tolerance induction in human dMo. We also propose that persistent metabolism of glucose to lactate in aerobic conditions is essential for the generation of human $1,25D_3$-DCs. This metabolic pathway can provide the necessary carbons to fuel the energy demand for the massive cytoskeletal-membrane rearrangements occurring during human DC maturation in the presence of $1,25(OH)_2D_3$ (Ferreira et al., 2012; Ferreira et al., 2009). The DC cytoskeletal structures determine cell shape, function, and fate.

The PI3K/Akt/mTOR pathway was also shown to be central in inducing and maintaining the tolerogenic properties of $1,25D_3$-DCs. This combined metabolic effect of $1,25(OH)_2D_3$ in human DCs is quite unique in literature. Thus, our findings contrast with previous reports linking glycolysis and the PI3K/Akt/mTOR pathway to the induction of a proinflammatory profile in murine DCs and T cells (Dang et al., 2011; Krawczyk et al., 2010; Michalek et al., 2011; Shi et al., 2011). On the other hand, recent data indicate that murine T cell proliferation/survival is largely dependent on OXPHOS, not requiring a switch to aerobic glycolysis (Pearce and Pearce, 2013). In addition, FoxP3 gene expression, a classical Treg marker, is controlled by HIF-1α signaling via mTOR (Clambey et al., 2012), thus demonstrating the importance of this pathway in the function of Tregs (Zeng et al., 2013). Finally, effector T cells have increased OXPHOS in conjunction with glycolysis, which is maintained even after achieving full activation (Sena et al., 2013; van der Windt et al., 2012; Wang and Green, 2012).

This particular metabolic profile induced by $1,25(OH)_2D_3$ in DCs determines their tolerogenic phenotype and function, as the tolerogenic properties of these cells could only be fully established when glucose is available and the PI3K/Akt/mTOR pathway is functional. In addition, the amount of available glucose, especially at the start of the differentiation process from human monocytes, is essential for the development of $1,25D_3$-DCs. Nutrient deprivation itself may interfere with this tolerogenic network through decreasing ATP levels. The resulting increased AMP/ATP ratio is then sensed by AMPK, which, in turn, phosphorylates TSC2, inhibiting mTOR downstream from PI3K and Akt (Figure 7C; Dang, 2012). Finally, culturing DCs in low oxygen concentrations only had a limited impact on the phenotype of $1,25D_3$-DCs, whereas no impairment of their tolerogenic function was observed. This suggests that the increase in glucose oxidation and in the expression of OXPHOS-related genes by $1,25(OH)_2D_3$ is not an underlying cause for the induction and maintenance of the observed tolerogenic DC phenotype. Because $1,25D_3$-DCs have been shown to migrate in vivo and exert their function in sites of inflammation where oxygen may be limiting (Ferreira et al., 2014), the fact that hypoxia does not change their tolerogenic function is an important observation.

Most importantly, our data show that PI3K and its downstream pathway are essential not only for maintenance of the $1,25D_3$-DC phenotype, but also for their functional impact on T cells. We hypothesize that vitamin D receptor (VDR)-bound $1,25(OH)_2D_3$ acts via the PI3K/Akt/mTOR pathway to control the expression of different cell-surface molecules (Bocelli-Tyndall et al., 2010) and the balance between the production of immunomodulatory and proinflammatory cytokines (Belladonna et al., 2008; Wang et al., 2011) (Figure 7C). Indeed, preliminary data in DCs

Figure 6. The PI3K/Akt/mTOR Axis Is Essential for the Induction and Maintenance of the Tolerogenic Phenotype in $1,25(OH)_2D_3$-Modulated DCs

(A) Simplified representation of the PI3K-Akt-mTOR pathway illustrating target proteins of the small molecule inhibitors (LY294002 and RAPA) and activators (AICAR) used.

(B) Human Ctr- or $1,25D_3$-DCs were obtained in vitro in the presence of 1.5 μM LY294002, 10 nM RAPA, 0.1 mM AICAR, or vehicle. The DCs were then analyzed by FACS to detect their surface expression of different markers (CD86, HLA-DR, CD80) ($n = 4–13$; $^*p < 0.05$, $^{**}p < 0.01$, $^{***}p < 0.001$, $^{****}p < 0.0001$). Values depicted in the bar graph represent average MFI levels ± SEM from surface molecules analyzed in Ctr- or $1,25D_3$-DCs cultured in the presence of vehicle, LY294002, RAPA, or AICAR. ELISA was used to analyze the release of the cytokines IL-10 and IL-12p70 to the culture medium, and the values were then expressed as the ratio IL-10/IL-12p70 ($n = 3–5$; $^{**}p < 0.01$, $^{***}p < 0.001$). Glucose content of DC culture supernatants measured at the end of the differentiation/maturation period ($n = 3–7$, $^*p < 0.05$, $^{***}p < 0.001$, $^{****}p < 0.0001$).

(C) Schematic representation of the DC differentiation/maturation process from $CD14^+$ monocytes (6 days in culture during the differentiation period from monocytes to iDCs; 2 days in culture during the maturation period, as mentioned in Experimental Procedures). The strategy regarding the use of tolerogenic compounds is indicated in the figure.

(D) Ctr- and variously treated tolDCs (with DEX, ITF2357, RAPA or IL-10), cultured in the presence or in the absence of 1.5 μM LY294002, were analyzed for their surface marker expression, cytokine release to the medium, and media glucose content as described in (A) ($n = 4–13$).

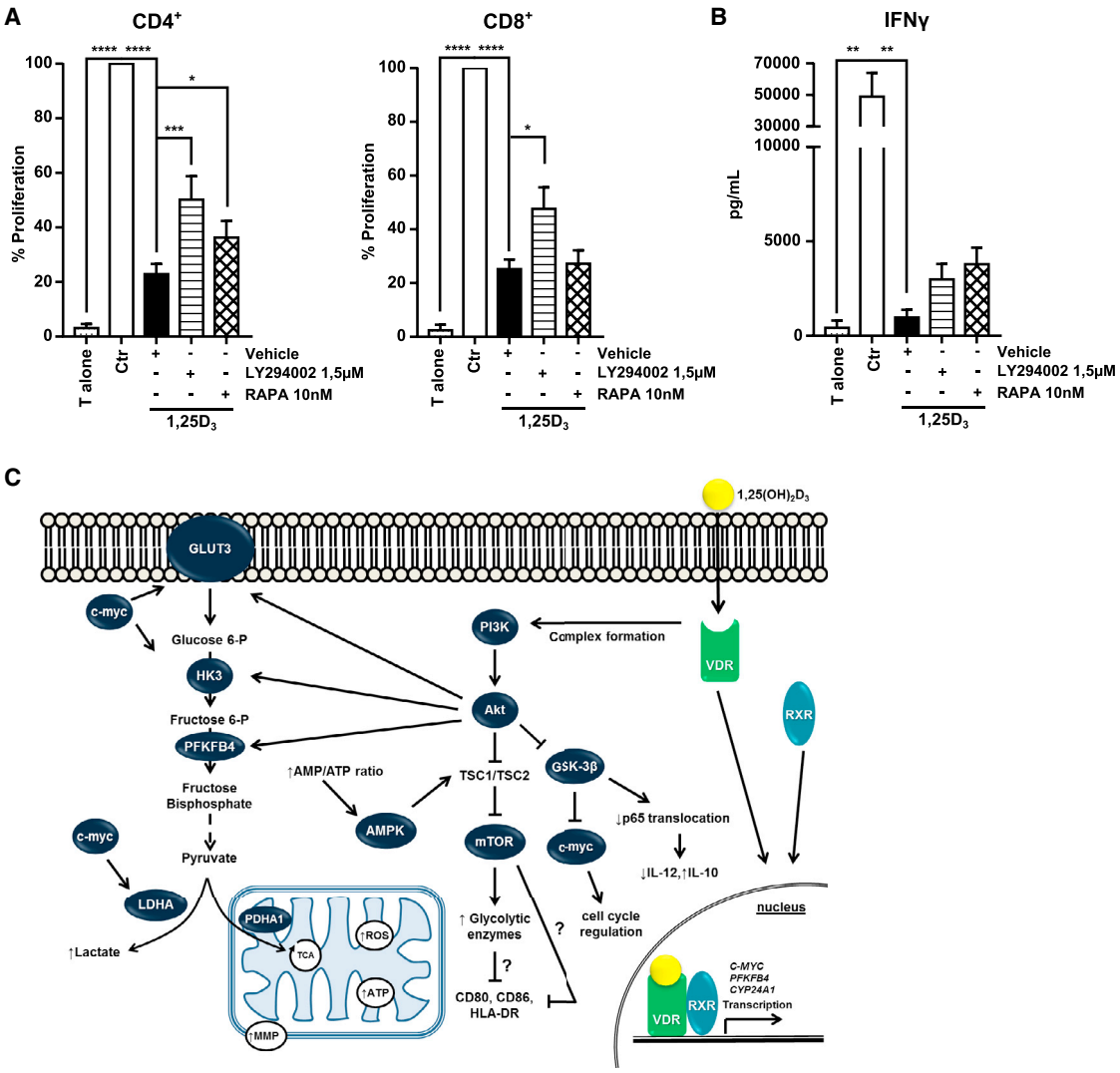

Figure 7. Inhibition of the PI3K/Akt/mTOR Reverses the Tolerogenic Function of $1,25(OH)_2D_3$-Modulated DCs

Allogeneic total $CD3^+$ T cells were isolated from healthy donors, labeled with the eFluor670 cell proliferation dye, and cocultured in vitro in the presence of Ctr-, vehicle-$1,25D_3$-, LY294002-$1,25D_3$-, or RAPA-$1,25D_3$-DCs.

(A) Proliferation of labeled T cells was analyzed after 4 days in coculture by means of eFluor670 cell proliferation dye dilution. The results are expressed as percentage ± SEM of proliferation inhibition of $CD4^+$ (left) or $CD8^+$ (right) T cells, with proliferation in the presence of Ctr-DCs set as 100% ($n = 6$; $^{**}p < 0.01$, $^{****}p < 0.0001$).

(B) IFN-γ levels in culture supernatants of the DC:T cell cocultures ($n = 4$, $^{**}p < 0.01$).

(C) Proposed model for the mechanism of action of $1,25(OH)_2D_3$ in human-monocyte-derived DCs. We hypothesize that VDR-bound $1,25(OH)_2D_3$ activates the PI3K-Akt-mTOR pathway via either forming a complex and phosphorylating the regulatory subunit of PI3K, or by other unknown mechanisms. This releases and activates the catalytic subunit, which unleashes the PI3K downstream pathway. Among other functions, activation of this pathway promotes the expression of different key glycolytic enzymes, which induces glycolysis. Control of surface marker expression and cytokine production by $1,25(OH)_2D_3$ might arise from its impact on the PI3K pathway, which can control essential transcription factors (e.g., GSK-3β and NF-κB nuclear translocation) or from the direct regulation of transcription factors, key metabolic bifunctional enzymes, and RNA binding proteins. In the absence of glucose or glycolysis, an increase in the AMP/ATP ratio will be sensed by AMPK, which, in turn, phosphorylates TSC2 and blocks activation of the mTOR complex and its downstream processes. We further consider that the increase in OXPHOS also seen in $1,25D_3$-DCs is derived from the excess pyruvate generated during induced glycolysis, in addition to the control of metabolic enzymes from the oxidative branch by $1,25(OH)_2D_3$.

generated from $VDR^{-/-}$ mice demonstrate that the phenotypic alterations induced by $1,25(OH)_2D_3$ in these cells are dependent on the VDR (data not shown). In line with this, treatment of primary human monocytes with $1,25(OH)_2D_3$ induces the formation of a signaling complex in which the VDR-bound $1,25(OH)_2D_3$ associates with p85, the regulatory subunit of the PI3K complex. This association is essential for $1,25(OH)_2D_3$-mediated expression of the monocyte surface markers CD14 and CD11b (Hmama et al., 1999). Under our experimental conditions, control of surface marker expression and cytokine production by

$1,25(OH)_2D_3$ might thus arise from its impact on the PI3K pathway, which can control essential transcription factors. A similar phenomenon has been previously suggested for the effects of GSK-3β on NF-κB nuclear translocation in LPS-stimulated monocytes (Wang et al., 2011). In addition, PI3K can also activate *C-MYC*, which plays an essential role in facilitating increased rates of glucose uptake and glycolysis (Jones and Thompson, 2009). Although *C-MYC* is downregulated by $1,25(OH)_2D_3$ in different tumors (Colston and Hansen, 2002; Heikkinen et al., 2011; Rohan and Weigel, 2009; Salehi-Tabar et al., 2012), the mRNA levels of this transcription factor are upregulated in human dMo by $1,25(OH)_2D_3$ already at 4 hr after the start of the treatment (present data). This may contribute to the observed increased levels of glycolytic enzymes, glucose transporters, and glycolysis in $1,25D_3$-DCs. Furthermore, control of the expression of key metabolic enzymes might represent an additional underlying mechanism by which $1,25(OH)_2D_3$ exerts its immunomodulatory effects on human DCs. This is in line with previous research suggesting that bifunctional enzymes and RNA binding proteins can coordinate metabolism and gene expression through RNA/enzyme/metabolite networks (Pearce et al., 2013) (Figure 7C).

In conclusion, we showed that glucose availability, glucose-derived carbon usage and a functional PI3K/Akt/mTOR pathway are essential to maintain the tolerogenic phenotype of $1,25D_3$-DCs. By limiting glucose concentrations in the medium and blocking the PI3K/Akt/mTOR pathway using small pharmacological inhibitors, we showed that tolDCs induced specifically by $1,25(OH)_2D_3$, but not by other tolerogenic compounds, are largely dependent on these features to maintain their tolerogenic phenotype and function. Although OXPHOS is thought to be a general process required for the induction of tolerance in immune cells, our data identify glycolysis and the PI3K-Akt-mTOR pathway as central regulators of the tolerogenic properties of $1,25(OH)_2D_3$-generated DCs. Importantly, after the metabolic reprogramming has taken place in $1,25D_3$-DCs, these cells will not depend on a normoxic environment or on normoglycemic conditions to survive and maintain phenotype. This will allow the re-educated cells to exert their immunomodulatory effects in vivo in the inhospitable environments where they will home to restore tolerance. We believe that these metabolic insights in tolerogenic DC biology are important to support the development of DC-based immunotherapies and to influence DC longevity and their resistance to environmental metabolic stress.

EXPERIMENTAL PROCEDURES

Detailed experimental procedures are provided in the Supplemental Information.

In Vitro Generation of Human-Monocyte-Derived DCs

Human DCs were obtained in vitro from freshly isolated monocytes as previously described (Ferreira et al., 2012), in accordance with the ethics committee of the KU Leuven (Figure S1). For inducing DC differentiation, isolated monocytes were cultured in differentiation media with 1,000 U/ml recombinant human IL-4 (Gentaur) and 800 U/ml recombinant human GM-CSF (Gentaur). Medium and cytokines were refreshed on day 3. On day 6, media was replenished and maturation was induced in the iDC cultures by 100 ng/ml LPS (Sigma), 1,000 U/ml recombinant human IFN-γ (Roche), and 800 U/ml GM-CSF (Gentaur).

Chemical Compound Treatment

$1,25(OH)_2D_3$ (10^{-8} M) (Sigma), dexamethasone (DEX, 10^{-6} M) (Panpharma), Givinostat (ITF2357, 100 nM) (Selleckchem/Divbio Science), and RAPA (10 ng/ml) (Roche) were added at the beginning of the culture at the indicated final concentrations and refreshed at day 3. Recombinant human IL-10 (40 ng/ml) (PeproTech) was added on day 6 of culture. DCA (5 mM) (Sigma), etomoxir (20 mM) (Calbiochem-EMD Millipore), LY294002 (1.5 μM) (Calbiochem-EMD Millipore), and AICAR (0.1 mM) (Calbiochem-EMD Millipore) were added every day to the DC cultures, 30 min before addition of tolerogenic compound or maturation stimulus. Similar dilutions of ethanol, DMSO, or PBS were used as vehicle controls.

Flow Cytometry Analysis of Human DC Surface Markers

Ctr- and $1,25D_3$-DCs were analyzed for their surface marker expression by fluorescence-activated cell sorting (FACS). All staining procedures were performed in PBS containing 2 mM EDTA and 0.1% BSA. Cells were preincubated with anti-CD16/CD32 to minimize nonspecific binding. Thereafter, 2.5×10^5 cells were labeled with the following conjugated antibodies: CD1a (from BioLegend), CD14 and HLA-DR (from Affymetrix/eBioscience), CD80 and CD86 (from BD Biosciences), and matching isotype controls. Signal height and widths were used to exclude doublets. Dead cells were excluded by using the Fixable Live/Dead Yellow stain according to the manufacturer's specifications (Invitrogen). Data acquisition was performed on a Gallios flow cytometer (Beckman Coulter Genomics), and the Kaluza software (Beckman Coulter) was used for data analysis.

Isolation of Allogeneic Human T Cells, In Vitro Lymphocyte Proliferation, and FACS Analysis

Purified $CD3^+$ T cells were prepared from peripheral blood mononuclear cells of healthy donors using the Pan T cell II kit (Miltenyi Biotec), according to the manufacturer's instructions. Purity was routinely 90%–95%, as assessed by FACS. Purified allogeneic $CD3^+$ T cells were labeled with the eFluor670 Proliferation Dye (Affymetrix/eBioscience) and cocultured with (extensively washed) DCs at a 1:10–50 DC:T cell ratio. Cells were cultured for 4 days before antibody staining and FACS analysis. T cell proliferation was assessed by simultaneous staining for CD4 and CD8 (from Affymetrix/eBioscience). Cells were gated based on the forward and side scatter (lymphocyte gate) and signal height and widths (doublet exclusion). Further analysis was performed as described above.

Statistical Analysis

Data were tested for statistical significance using the paired t test, one sample t test, or one-way ANOVA with subsequent Tukey post-test for multiple comparisons, using the GraphPad Prism software. For all tests, data were considered significantly different at $p < 0.05$.

ACCESSION NUMBERS

The GEO accession number for the microarray data reported herein is GSE56490.

SUPPLEMENTAL INFORMATION

Supplemental Information includes Supplemental Experimental Procedures, six figures, and four tables and can be found with this article online at http://dx.doi.org/10.1016/j.celrep.2015.01.013.

ACKNOWLEDGMENTS

G.B.F. designed and performed experiments, analyzed data, and wrote the manuscript. A-S.V., A.C.F.G., L.V.L., L.V., M.G., and T.N. designed and performed experiments and analyzed data. G.E., K.M., A.V., C.G., P.C., F.S., and D.L.E. designed experiments, analyzed data, and wrote the manuscript. C.M. and L.O. supervised the project, designed experiments, and wrote the manuscript.

The technical experience of Anyishaï Z. Musuaya, Elien De Smidt, Frea Coun, Omer Rutgeerts, and Wim Cockx is greatly appreciated. The authors

would like to thank Drs. D. Rondas and W. D'Hertog for fruitful scientific discussions. This work was supported by grants from the Flemish Research Foundation (G.0649.08 and G.0734.10, a postdoctoral fellowship to G.B.F., and a clinical fellowship to C.M.), the Belgium Program on Interuniversity Poles of Attraction initiated by the Belgian State (P6/40), the Katholieke Universiteit Leuven (GOA 2009/10 and GOA 14/010), and the 7th Framework Program of the European Union (NAIMIT).

Received: April 4, 2014
Revised: November 21, 2014
Accepted: December 31, 2014
Published: February 5, 2015

REFERENCES

Belladonna, M.L., Volpi, C., Bianchi, R., Vacca, C., Orabona, C., Pallotta, M.T., Boon, L., Gizzi, S., Fioretti, M.C., Grohmann, U., and Puccetti, P. (2008). Cutting edge: Autocrine TGF-beta sustains default tolerogenesis by IDO-competent dendritic cells. J. Immunol. *181*, 5194–5198.

Bocelli-Tyndall, C., Zajac, P., Di Maggio, N., Trella, E., Benvenuto, F., Iezzi, G., Scherberich, A., Barbero, A., Schaeren, S., Pistoia, V., et al. (2010). Fibroblast growth factor 2 and platelet-derived growth factor, but not platelet lysate, induce proliferation-dependent, functional class II major histocompatibility complex antigen in human mesenchymal stem cells. Arthritis Rheum. *62*, 3815–3825.

Clambey, E.T., McNamee, E.N., Westrich, J.A., Glover, L.E., Campbell, E.L., Jedlicka, P., de Zoeten, E.F., Cambier, J.C., Stenmark, K.R., Colgan, S.P., and Eltzschig, H.K. (2012). Hypoxia-inducible factor-1 alpha-dependent induction of FoxP3 drives regulatory T-cell abundance and function during inflammatory hypoxia of the mucosa. Proc. Natl. Acad. Sci. USA *109*, E2784–E2793.

Colston, K.W., and Hansen, C.M. (2002). Mechanisms implicated in the growth regulatory effects of vitamin D in breast cancer. Endocr. Relat. Cancer *9*, 45–59.

Dang, C.V. (2012). Links between metabolism and cancer. Genes Dev. *26*, 877–890.

Dang, E.V., Barbi, J., Yang, H.Y., Jinasena, D., Yu, H., Zheng, Y., Bordman, Z., Fu, J., Kim, Y., Yen, H.R., et al. (2011). Control of T(H)17/T(reg) balance by hypoxia-inducible factor 1. Cell *146*, 772–784.

Delmastro-Greenwood, M.M., and Piganelli, J.D. (2013). Changing the energy of an immune response. Am. J. Clin. Exp. Immunol. *2*, 30–54.

Everts, B., Amiel, E., van der Windt, G.J., Freitas, T.C., Chott, R., Yarasheski, K.E., Pearce, E.L., and Pearce, E.J. (2012). Commitment to glycolysis sustains survival of NO-producing inflammatory dendritic cells. Blood *120*, 1422–1431.

Everts, B., Amiel, E., Huang, S.C., Smith, A.M., Chang, C.H., Lam, W.Y., Redmann, V., Freitas, T.C., Blagih, J., van der Windt, G.J., et al. (2014). TLR-driven early glycolytic reprogramming via the kinases TBK1-IKKε supports the anabolic demands of dendritic cell activation. Nat. Immunol. *15*, 323–332.

Ferreira, G.B., van Etten, E., Lage, K., Hansen, D.A., Moreau, Y., Workman, C.T., Waer, M., Verstuyf, A., Waelkens, E., Overbergh, L., and Mathieu, C. (2009). Proteome analysis demonstrates profound alterations in human dendritic cell nature by TX527, an analogue of vitamin D. Proteomics *9*, 3752–3764.

Ferreira, G.B., Kleijwegt, F.S., Waelkens, E., Lage, K., Nikolic, T., Hansen, D.A., Workman, C.T., Roep, B.O., Overbergh, L., and Mathieu, C. (2012). Differential protein pathways in 1,25-dihydroxyvitamin d(3) and dexamethasone modulated tolerogenic human dendritic cells. J. Proteome Res. *11*, 941–971.

Ferreira, G.B., Gysemans, C.A., Demengeot, J., da Cunha, J.P., Vanherwegen, A.S., Overbergh, L., Van Belle, T.L., Pauwels, F., Verstuyf, A., Korf, H., and Mathieu, C. (2014). 1,25-Dihydroxyvitamin D3 Promotes Tolerogenic Dendritic Cells with Functional Migratory Properties in NOD Mice. J Immunol.

Frauwirth, K.A., and Thompson, C.B. (2004). Regulation of T lymphocyte metabolism. J. Immunol. *172*, 4661–4665.

Heikkinen, S., Väisänen, S., Pehkonen, P., Seuter, S., Benes, V., and Carlberg, C. (2011). Nuclear hormone 1α,25-dihydroxyvitamin D3 elicits a genome-wide shift in the locations of VDR chromatin occupancy. Nucleic Acids Res. *39*, 9181–9193.

Hmama, Z., Nandan, D., Sly, L., Knutson, K.L., Herrera-Velit, P., and Reiner, N.E. (1999). 1alpha,25-dihydroxyvitamin D(3)-induced myeloid cell differentiation is regulated by a vitamin D receptor-phosphatidylinositol 3-kinase signaling complex. J. Exp. Med. *190*, 1583–1594.

Jones, R.G., and Thompson, C.B. (2009). Tumor suppressors and cell metabolism: a recipe for cancer growth. Genes Dev. *23*, 537–548.

Kleijwegt, F.S., Laban, S., Duinkerken, G., Joosten, A.M., Koeleman, B.P., Nikolic, T., and Roep, B.O. (2011). Transfer of regulatory properties from tolerogenic to proinflammatory dendritic cells via induced autoreactive regulatory T cells. J. Immunol. *187*, 6357–6364.

Krauss, S., Brand, M.D., and Buttgereit, F. (2001). Signaling takes a breath—new quantitative perspectives on bioenergetics and signal transduction. Immunity *15*, 497–502.

Krawczyk, C.M., Holowka, T., Sun, J., Blagih, J., Amiel, E., DeBerardinis, R.J., Cross, J.R., Jung, E., Thompson, C.B., Jones, R.G., and Pearce, E.J. (2010). Toll-like receptor-induced changes in glycolytic metabolism regulate dendritic cell activation. Blood *115*, 4742–4749.

Locasale, J.W., and Cantley, L.C. (2011). Genetic selection for enhanced serine metabolism in cancer development. Cell Cycle *10*, 3812–3813.

Michalek, R.D., Gerriets, V.A., Jacobs, S.R., Macintyre, A.N., MacIver, N.J., Mason, E.F., Sullivan, S.A., Nichols, A.G., and Rathmell, J.C. (2011). Cutting edge: distinct glycolytic and lipid oxidative metabolic programs are essential for effector and regulatory CD4+ T cell subsets. J. Immunol. *186*, 3299–3303.

Pearce, E.L., and Pearce, E.J. (2013). Metabolic pathways in immune cell activation and quiescence. Immunity *38*, 633–643.

Pearce, E.L., Poffenberger, M.C., Chang, C.H., and Jones, R.G. (2013). Fueling immunity: insights into metabolism and lymphocyte function. Science *342*, 1242454.

Rohan, J.N., and Weigel, N.L. (2009). 1Alpha,25-dihydroxyvitamin D3 reduces c-Myc expression, inhibiting proliferation and causing G1 accumulation in C4-2 prostate cancer cells. Endocrinology *150*, 2046–2054.

Salehi-Tabar, R., Nguyen-Yamamoto, L., Tavera-Mendoza, L.E., Quail, T., Dimitrov, V., An, B.S., Glass, L., Goltzman, D., and White, J.H. (2012). Vitamin D receptor as a master regulator of the c-MYC/MXD1 network. Proc. Natl. Acad. Sci. USA *109*, 18827–18832.

Sena, L.A., Li, S., Jairaman, A., Prakriya, M., Ezponda, T., Hildeman, D.A., Wang, C.R., Schumacker, P.T., Licht, J.D., Perlman, H., et al. (2013). Mitochondria are required for antigen-specific T cell activation through reactive oxygen species signaling. Immunity *38*, 225–236.

Shaw, R.J., and Cantley, L.C. (2006). Ras, PI(3)K and mTOR signalling controls tumour cell growth. Nature *441*, 424–430.

Shi, L.Z., Wang, R., Huang, G., Vogel, P., Neale, G., Green, D.R., and Chi, H. (2011). HIF1alpha-dependent glycolytic pathway orchestrates a metabolic checkpoint for the differentiation of TH17 and Treg cells. J. Exp. Med. *208*, 1367–1376.

Széles, L., Keresztes, G., Töröcsik, D., Balajthy, Z., Krenács, L., Póliska, S., Steinmeyer, A., Zuegel, U., Pruenster, M., Rot, A., and Nagy, L. (2009). 1,25-dihydroxyvitamin D3 is an autonomous regulator of the transcriptional changes leading to a tolerogenic dendritic cell phenotype. J. Immunol. *182*, 2074–2083.

Unger, W.W., Laban, S., Kleijwegt, F.S., van der Slik, A.R., and Roep, B.O. (2009). Induction of Treg by monocyte-derived DC modulated by vitamin D3 or dexamethasone: differential role for PD-L1. Eur. J. Immunol. *39*, 3147–3159.

van der Windt, G.J., Everts, B., Chang, C.H., Curtis, J.D., Freitas, T.C., Amiel, E., Pearce, E.J., and Pearce, E.L. (2012). Mitochondrial respiratory capacity is a critical regulator of CD8+ T cell memory development. Immunity *36*, 68–78.

van Halteren, A.G., van Etten, E., de Jong, E.C., Bouillon, R., Roep, B.O., and Mathieu, C. (2002). Redirection of human autoreactive T-cells Upon interaction with dendritic cells modulated by TX527, an analog of 1,25 dihydroxyvitamin D(3). Diabetes *51*, 2119–2125.

van Halteren, A.G., Tysma, O.M., van Etten, E., Mathieu, C., and Roep, B.O. (2004). 1alpha,25-dihydroxyvitamin D3 or analogue treated dendritic cells modulate human autoreactive T cells via the selective induction of apoptosis. J. Autoimmun. *23*, 233–239.

Vats, D., Mukundan, L., Odegaard, J.I., Zhang, L., Smith, K.L., Morel, C.R., Wagner, R.A., Greaves, D.R., Murray, P.J., and Chawla, A. (2006). Oxidative metabolism and PGC-1beta attenuate macrophage-mediated inflammation. Cell Metab. *4*, 13–24.

Wang, R., and Green, D.R. (2012). Metabolic checkpoints in activated T cells. Nat. Immunol. *13*, 907–915.

Wang, H., Brown, J., Gu, Z., Garcia, C.A., Liang, R., Alard, P., Beurel, E., Jope, R.S., Greenway, T., and Martin, M. (2011). Convergence of the mammalian target of rapamycin complex 1- and glycogen synthase kinase 3-β-signaling pathways regulates the innate inflammatory response. J. Immunol. *186*, 5217–5226.

Williams, A., Henao-Mejia, J., Harman, C.C., and Flavell, R.A. (2013). miR-181 and metabolic regulation in the immune system. Cold Spring Harb. Symp. Quant. Biol. *78*, 223–230.

Zeng, H., Yang, K., Cloer, C., Neale, G., Vogel, P., and Chi, H. (2013). mTORC1 couples immune signals and metabolic programming to establish T(reg)-cell function. Nature *499*, 485–490.